Numerical Methods in Civil Engineering

Prediction of effective moment of inertia for hybrid FRP-steel reinforced concrete beams using the genetic algorithm

Ali Kheyroddin*, Fahimeh Maleki**

ARTICLE INFO

Article history:
Received:
February 2017.
Revised:
April 2017.
Accepted:
June 2017.

Keywords:
Hybrid RC beam,
Genetic algorithm,
Effective moment of Inertia,
FRP bars,
Deflection.

Abstract:

The use of Concrete beams reinforced with a combination of fiber reinforced polymer (FRP) and steel bars has increased dramatically in recent years, due to improvement in strength and flexural ductility simultaneously. In this paper, we proposed a new equation for estimating the effective moment of inertia of hybrid FRP-steel reinforced concrete (RC) beams on the basis of the genetic algorithm and experimental results.The genetic algorithm is used to optimize the percent error between experimental and analytical responses. In the proposed equation, additional coefficients are considered in order to take into account the specific properties of FRP bars. The effects of the elastic modulus of FRP and steel bars, the hybrid reinforcement ratio, A_f /A_s, and the different level of loading on the effective moment of inertia has been considered.These coefficients are used to modify Branson's equation to compute the effective moment of inertia of concrete beams reinforced by FRP and steel bars. Comparison between the experimental and predicted results showed the adequacy of the model used in predicting the effective moment of inertia, and deflection of hybrid – RC beams.

1. Introduction

The use of fiber reinforced polymer (FRP) bars in structural concrete has rapidly increased in the last two decades due to their superior durability, excellent corrosion resistance, nonmagnetic properties, and high strength-to-weight ratio compared to conventional steel bars. On the other hand, FRP bars have a lower modulus of elasticity compared to steel. Due to this fact, the same amount of reinforcement exhibits larger deflections and crack widths in FRP reinforced concrete beams than in steel reinforced concrete beams. Hence, the design of such beams is typically governed by the serviceability limit state, which makes accurate determination of deflection extremely important (Dundar et al 2015[1]).

Despite the aforementioned advantages, FRP exhibits a linear elastic behaviour up to failure and possesses no ductility in general compared to conventional steel bars, which is considered a drawback when it serves as an internal reinforcement in concrete structures (Aiello & Ombres 2002[2]; Masmoudi et al 1998[3]; Kocaoz et al 2005[4]). In order to increase the ductility of FRP reinforced concrete (FRPRC) flexural members, many researchers have experimentally investigated the design of adding longitudinal steel bars to FRPRC beams (Bakis et al 2001[5]; Jo et al 2004[6]; Newhook 2000[7]; Acciai et al 2016[8]; Kara et al 2013[9]; Ge et al 2015[10]; Qu et al 2009[11]). With the addition of the steel bars, the ductility of hybrid FRPRC beam is significantly improved compared to that of pure FRPRC beam. Such ductility improvement is essential because it can provide ample warning before structural collapse, especially when the structure is under

** Corresponding Author: Professor, Department of Civil Engineering, Semnan University, Semnan, Iran. Email: kheyroddin@semnan.ac.ir*
*** MSc student, Department of Civil Engineering, Semnan University, Semnan, Iran. Email: f-maleki@semnan.ac.ir*

seismic attack. Furthermore, the additional steel bars can ensure that the ductile behavior of flexural member is maintained. In hybrid reinforcement scenario, the strength is mainly provided by FRP reinforcement and the ductility is provided by the addition of steel reinforcement. Since the additional steel reinforcement is not designed for load bearing capacity of the beam, a certain extent of steel corrosion could be acceptable, especially in an aggressive environment. The optimized structural performance can be achieved by designing the hybrid reinforcement appropriately (Ge et al 2015[10]; Qu et al 2009[11]). Consequently, a method is needed to predict the expected service load deflection of hybrid FRP / steel reinforced concrete beams with a reasonably high degree of accuracy.

The principle goal of this study is to propose a new model for prediction of effective moment of inertia in hybrid concrete beams based on genetic algorithm and then justify it against experimental data and existing models. One hundred twenty data points have been applied to obtain the equation.

2. Existing models for effective moment of inertia calculation:

For FRP reinforced beams, the balance reinforcement ratio refers to a simultaneous rupture of FRP bars and concrete crushing. The balance ratio, ρ_{fb}, is therefore determined by Eq. (1).

$$\rho_{fb} = 0.85\beta_1 \frac{f_c'}{f_{fu}} \frac{E_f \varepsilon_{cu}}{E_f \varepsilon_{cu} + f_{fu}} \quad (1)$$

Where E_f and f_{fu} are the modulus of elasticity and ultimate tensile stress of FRP bars, β1 is the ratio of the depth of equivalent rectangular stress block to the depth of the neutral axis, f_c' and ε_{cu} are the concrete compressive strength and maximum concrete compressive strain, respectively.

The effective reinforcement ratio, ρ_{eff}, for hybrid reinforced beams is determined using Eq. (2). This ratio is compared to the balance ratio of the FRP reinforcement, to define the expected failure mode in each hybrid beam. If $\rho_{eff} > \rho_{fb}$, then beam is over reinforced and the flexural failure is expected to occur due to concrete crushing. If $\rho_{eff} \leq \rho_{fb}$, then the beam is under reinforced and steel bars are expected to yield prior to concrete crushing (El Refai et al 2015[12]).

$$\rho_{eff} = \frac{A_s \frac{f_y}{f_{fu}} + A_f}{bd} = \rho_s \frac{f_y}{f_{fu}} + \rho_f \quad (2)$$

Where A_s and A_f are the area of steel and area of FRP reinforcement, respectively. f_y is the yield stress in steel reinforcement. b is the width of the cross section; d is the distance from the extreme fiber in compression to the center of reinforcement. ρ_f and ρ_s are FRP reinforcement ratio and steel reinforcement ratio respectively.

For hybrid-RC beams, various failure modes directly affect the performance of members. The effective reinforcement stiffness $\rho_{sf,s}$ and the mechanical reinforcing index $\rho_{sf,f}$ are calculated by Eqs. (3) and (4) (Pang et al 2015[13]):

$$\rho_{sf,s} = \frac{E_s A_s + E_f A_f}{E_s bd} = \rho_s + \frac{E_f}{E_s}\rho_f \quad (3)$$

$$\rho_{sf,f} = \frac{f_y A_s + f_{fu} A_f}{f_{fu} bd} = \rho_s \frac{f_y}{f_{fu}} + \rho_f \quad (4)$$

The yield reinforcement ratio ρ_{sb} can be calculated as the reinforcement ratio when concrete crushing and steel yielding occur simultaneously but the FRP bars have not yet ruptured. The ρ_{fb} can be calculated as the reinforcement ratio when concrete crushing and FRP bar rupturing occur simultaneously after the steel rebars have yielded (Pang et al 2015[13]). ρ_{sb} calculated by Eq. (5):

$$\rho_{sb} = 0.85\beta_1 \frac{f_c'}{f_y} \frac{E_s \varepsilon_{cu}}{f_y + E_s \varepsilon_{cu}} \quad (5)$$

Results show that when the mechanical reinforcing index, $\rho_{sf,f}$, is greater than the critical reinforcement ratio, ρ_{fb}, and the effective reinforcement stiffness, $\rho_{sf,s}$, is less than the yield reinforcement ratio, ρ_{sb}, flexural failure of the beam will begin with steel yielding followed by concrete crushing and eventually FRP bar rupturing. The section is under-reinforced, which is a preferred approach in the design of hybrid-RC members (Pang et al 2015[13]). Under-reinforced beam design can be adopted as an economical method in hybrid RC design. However, the load-carrying capacity of under-reinforced design is generally lower since beams fail through rupture of FRP reinforcement and concrete does not reach its material limit. Ductility improvement can be achieved by steel yielding in under-reinforced hybrid RC beam at the expense of strength. In order to prevent excessive elongation that may cause the rupture of FRP reinforcement, the amount of FRP reinforcement should be larger than that of steel reinforcement. Thus, it is recommended that the over-reinforced beam design be adopted in hybrid RC beam design. It should be noticed that the hybrid reinforcement ratio, A_f/A_s, should be designed larger than 1 to ensure the strength of hybrid RC beam after yielding of steel reinforcement. However, this ratio should be smaller than 2.5 to meet the ductility requirement in normal service conditions with a reasonable stiffness and deformation resistance (Qin et al 2017[14]).

The effective moment of inertia (I_e), according to Branson's equation (1968) [15], can be calculated by Eq. (6), which is used to determine the deflection of steel reinforced beams, at service loads.

$$I_e = \left(\frac{M_{cr}}{M_a}\right)^3 I_g + \left[1 - \left(\frac{M_{cr}}{M_a}\right)^3\right] I_{cr} \leq I_g \quad (6)$$

Where M_a is applied moment at the critical section, M_{cr} is cracking moment, I_g and I_{cr} are the gross moment of inertia and cracked moment of inertia, respectively.

Previous studies concluded that Bransons' s equation overestimated effective moment of inertia of FRP reinforced beams, especially when the beams were under reinforcement (Yost et al 2003[16]). As demonstrated by Bischoff (2005) [17], Branson' s equation overestimates member stiffness when the I_g/I_{cr} of the member is greater than approximately three or four.

Kheyroddin and Mirza (1995) [18, 19] proposed a new equation for estimating of flexural rigidity, EI, of reinforced concrete beams. The compression reinforcement ratio and the compressive strength of concrete have a significant effect on the EI values for heavily reinforced beams and this effect decreases with a decrease in the tension reinforcement ratio. At the same level of moment, the flexural rigidity for beams loaded at mid span was found to be 18 percent more than that for beams subjected to uniformly distributed load. The effect of loading type on the EI value for heavily reinforced beams is not as significant as that of the lightly reinforced beams. The proposed equation takes into account the effect of the tension and compression reinforcement ratios, concrete compressive strength and the type of loading.

Shayanfar et al. (1997) [20] proposed Eq. (7) for eliminating the dependence of the computed results on the finite element size. In particular, the new model can be used effectively with relatively coarse finite element meshes with reasonable accuracy.

$$\varepsilon_{tu} = 0.004\, e^{-0.008h} \qquad (\varepsilon_{tu} \geq \varepsilon_{cr}) \quad (7)$$

If ε_{tu} is smaller than ε_{cr}, then

$$\varepsilon_{tu} = \varepsilon_{cr} \quad (8)$$

Where h is the width of the element (mm), (for non-square elements: h=$\sqrt{}$A, where A is the element area) and ε_{tu} is the concrete ultimate tensile strain. The proposed model exhibits good compatibility with the experimental results.

Bischoff (2007) [21] recommended a new expression for the effective moment of inertia I_e that showed appropriate agreement with test results for both steel and FRP reinforced concrete beams that could be computed from Eq. (9) below:

$$I_e = \frac{I_{cr}}{1-\eta(M_{cr}/M_a)^2} \leq I_g \quad (9)$$

$$\eta = 1 - \frac{I_{cr}}{I_g} \quad (10)$$

This equation is claimed to be equally applicable for FRP and steel RC beams.

Therefore, the ACI 440.1R-15 (2015) [22] committee introduced an additional factor γ, in expression proposed by Bischoff to account for the variation in stiffness along the length of the beams and could be determined by Eq. (11) as follows.

$$I_e = \frac{I_{cr}}{1-\gamma\left(\frac{M_{cr}}{M_a}\right)^2\left[1-\frac{I_{cr}}{I_g}\right]} \leq I_g \;\; where\; M_a \geq M_{cr} \quad (11)$$

The factor γ is dependent on load and boundary condition and accounts for the length of the uncracked regions of the member and for the change in stiffness in the cracked regions. The factor can be considered as Eq. (12), which is the result from integrating the curvature over the length of a simply supported beam with a uniformly distributed load.

$$\gamma = 1.72 - 0.72(M_{cr}/M_a) \quad (12)$$

The cracking moment M_{cr} is as specified in ACI 318 and should be computed using Eq. (13) as follows:

$$M_{cr} = \frac{0.62\,\lambda\sqrt{f_c'}\,I_g}{y_t} \quad (13)$$

Where y_t is distance from centroidal axis of gross section, neglecting reinforcement, to tension face and λ is modification factor reflecting the reduced mechanical properties of light weight concrete.

Benbokrane et al. (1996) [23] proposed Eq. (14), which was calibrated using a limited number of tests.

$$I_e = \alpha_0 I_{cr} + \left(\frac{I_g}{\beta_0} - \alpha_0 I_{cr}\right)\left[\frac{M_{cr}}{M_a}\right]^3 \quad (14)$$

Where α_0 and β_0 are equal to 0.84 and 7, respectively. The factor α_0 can reflect the reduced composite action between the concrete and FRP rebars. The factor β_0 was introduced in the equation to enable a faster transition from I_g to I_{cr}, since the degradation in stiffness due to the 3rd power component was considered to be too low.

Similar to Branson' s equation, the equations that were proposed by Mousavi et al. (2012) [24], the effective

moment of inertia, can be calculated using Equations as follows.

The objective function of model A has been defined by Eq. (15)

$$e = \left|\delta_{exp} - \delta_{cal}\right| \quad (15)$$

Model A is defined by Eqs. (16) and (17) as follows.

$$(I_e)_{Model\,A} = 0.15\left(\frac{M_{cr}}{M_a}\right)^m I_g + 0.89\left[1-\left(\frac{M_{cr}}{M_a}\right)^m\right] I_{cr} \le I_g \quad (16)$$

$$m = 0.66 - 0.3\frac{\rho_f}{\rho_{fb}} + 1.94\frac{M_{cr}}{M_a} + 4.64\frac{E_f}{E_s} \quad (17)$$

The objective function of model B has been defined by Eq. (18)

$$e = \left|(I_e)_{exp} - (I_e)_{theo}\right| \quad (18)$$

Model B is defined by Eqs. (19) and (20) as follows.

$$(I_e)_{Model\,B} = 0.17\left(\frac{M_{cr}}{M_a}\right)^m I_g + 0.94\left[1-\left(\frac{M_{cr}}{M_a}\right)^m\right] I_{cr} \le I_g \quad (19)$$

$$m = 1.69 - 0.51\frac{\rho_f}{\rho_{fb}} + 1.77\frac{M_{cr}}{M_a} + 6.67\frac{E_f}{E_s} \quad (20)$$

For beams tested under four-point loadings, the mid span deflection is determined using Eq. (21) as follows:

$$\Delta_{max} = \frac{P.L_a}{48E_cI_e}(3L^2 - 4L_a^2) \quad (21)$$

Where P is applied load, L_a is distance between the support and the point load (shear span), E_c is modulus of elasticity of concrete, L is beam length and Δ_{max} is maximum deflection at mid span of the beam.

On the other hand, the CSA-S806-12 (2012) [25] code recommends the use of the closed form relationship given in Eq. (22) to determine the maximum deflection of a beam loaded in four-point configuration. The rigidity of the beam is taken as $E_c I_{cr}$.

$$\Delta_{max} = \frac{P.L^3}{48\,E_cI_{cr}}\left[3\left(\frac{L_a}{L}\right) - 4\left(\frac{L_a}{L}\right)^3 - 8\eta\left(\frac{L_g}{L}\right)^3\right] \quad (22)$$

The parameter L_g represents the distance from the support to the point where M = M_{cr} and is determined as given in Eq. (23), η is coefficient given in Eq. (8).

$$L_g = L_a\frac{M_{cr}}{M_a} \quad (23)$$

In above equations, the cracked moment of inertia, I_{cr}, is determined from the elastic cracked section analysis as given in Eq. (24):

$$I_{cr} = \frac{1}{3}b(kd)^3 + \left(n_fA_f + n_sA_s\right)d^2(1-k)^2 \quad (24)$$

Where n_f is ratio of modulus of elasticity of FRP bars to modulus of elasticity of concrete, n_s is ratio of modulus of elasticity of steel bars to modulus of elasticity of concrete and k is coefficient and is determined as given in Eq. (25).

$$k = \sqrt{\left(n_f\rho_f + n_s\rho_s\right)^2 + 2\left(n_f\rho_f + n_s\rho_s\right)} - \left(n_f\rho_f + n_s\rho_s\right) \quad (25)$$

3. Genetic Algorithm (GA)

3.1 General

The genetic algorithm is a search based optimization technique based on evolutionary ideas of natural selection and genetics. The genetic algorithm is inspired by Darwin' s theory of evolution. Optimization in mathematical terms refers to maximizing or minimizing the objective function.

The genetic algorithms have been developed by John Holland, his colleagues, and his students at the University of Michigan. Genetic Algorithms (GAs) are different from more normal optimization and search procedures in four ways (Goldberg 1989[26]):

1. GAs work with a coding of the parameter set, not the parameters themselves.
2. GAs search from a population of points, not a single point.
3. GAs use payoff (objective function) information, not derivatives or other auxiliary knowledge.
4. GAs use probabilistic transition rules, not deterministic rules.

3.2 Encoding

Genetic algorithms deal with their encoded form instead of working on the parameters or problem variables. The genetic algorithm usually uses binary encoding. But in many cases, another encoding is required because of the nature of the problem. The types of encodings include binary, permutation, real number, and tree encoding. A schematic of the chromosome and its components are drawn in fig.1.

A string of bits is called a chromosome. In fact, the bits of a chromosome play the role of genes in nature. One of the main features of the genetic algorithms is that it alternates on the encoding space and the response space.

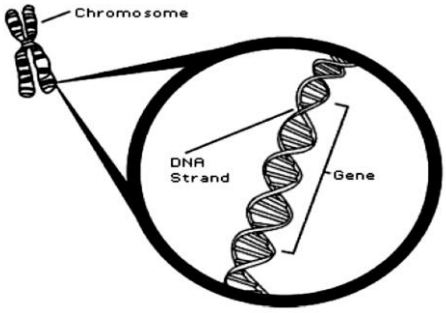

Fig.1: Schematic of a chromosome and its components

3.3 Initial population

After determining the encoding and displaying of the population, the first step is to create the initial population. This is usually done using random numbers generator, which distributes the number uniformly in the range desired in the chromosome string. In a different form of initial population generation, for each member of the population, a number of strings are generated and the string that has the highest efficiency in the fitness function is selected for that member.

3.4 Objective function and fitness function

However, in solving problems using the genetic algorithm, it is not necessary to know exactly the mathematical structure of the problem. But we should be able to measure the utility of each chromosome and its degree of compatibility in a way that, by eliminating the weaker answers, we can gradually approach the desired answer. In solving problems using the genetic algorithm, two steps can be followed. In the first step, each chromosome is evaluated by means of an objective function, which is often a mathematical function. Its input is a chromosome string consisting of decision variables and outputs are numbers that display the desired chromosome performance. The fitness function ultimately judges the fitness and compatibility of the response according to the amount of objective function.

3.5 Selection function

Selection is the component which guides the algorithm to the solution by preferring individuals with high fitness over low-fitted ones. It can be a deterministic operation, but in most implementations, it has random components (Bodenhofer 2003[27]).

3.6 Crossover operator

The most important operator in the genetic algorithm is the crossover operator. Crossover is a process in which the old generation of chromosomes combines to form a new generation of chromosomes. The pairs that were considered as the parent in the selection section will exchange their genes together and create new members. A crossover in the genetic algorithm results in the loss of the genetic diversity of the population because it allows the good genes to find each other. Fig.2. exhibits the single point crossover and the two-point crossover process.

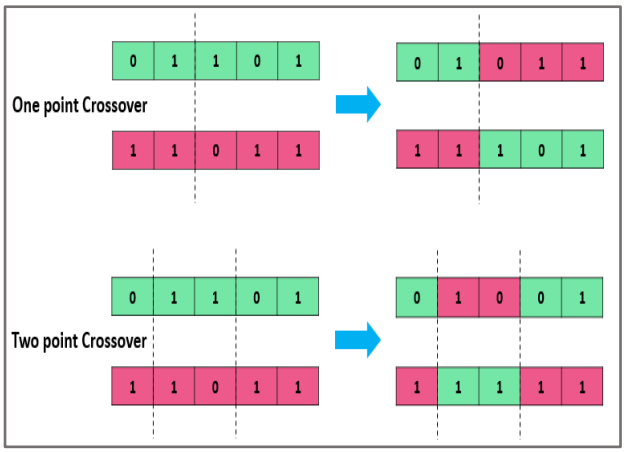

Fig.2: Crossover operator

3.7 *Mutation operator*

The next step is to apply random mutations. In nature, some factors such as UV rays, cause unpredictable changes in chromosomes. Since genetic algorithms follow the law of evolution, a low probability mutation operator can also be applied to these algorithms where the mutation searches for the intact spaces of the problem. It can be deduced that the most important duty of mutation is to avoid convergence to local optimality. The mutation process can be seen in Fig.3.

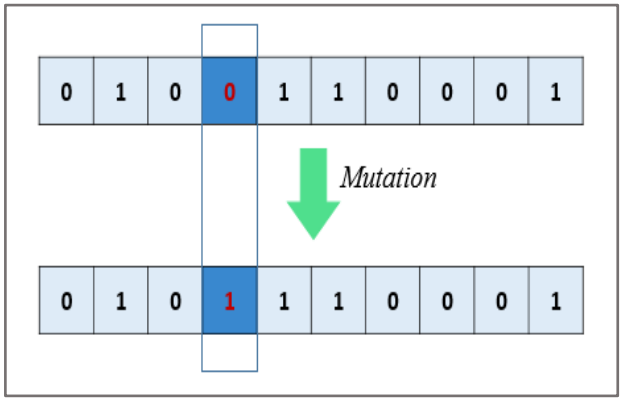

Fig.3: Mutation operator

3.8 Reinsertion

The reinsertion phase actually complements the selection, crossover and mutation steps. At this stage, the chromosomes, which should be replaced by new ones are identified.

The benefits of GA include the following:

Parallel processing is one of the most important advantages of the genetic algorithm. This means that in this method, instead of a variable, we grow a population to the optimal point at one time. So the convergence rate of the method is very high.

Because of the extent and dispersion of the points that are being searched, a good result is achieved in issues related to great search space.

A kind of targeted random search is considered, which produces different answers from different paths. In addition, there is no limit to the search and selection of random answers.

Because of the competition, the answer and selection of the best of the population, with a high probability to reach the optimal level, will be achieved.

Its implementation is simple and requires no complex problem-solving routines.

The general scheme of the genetic algorithm is shown in fig.4.

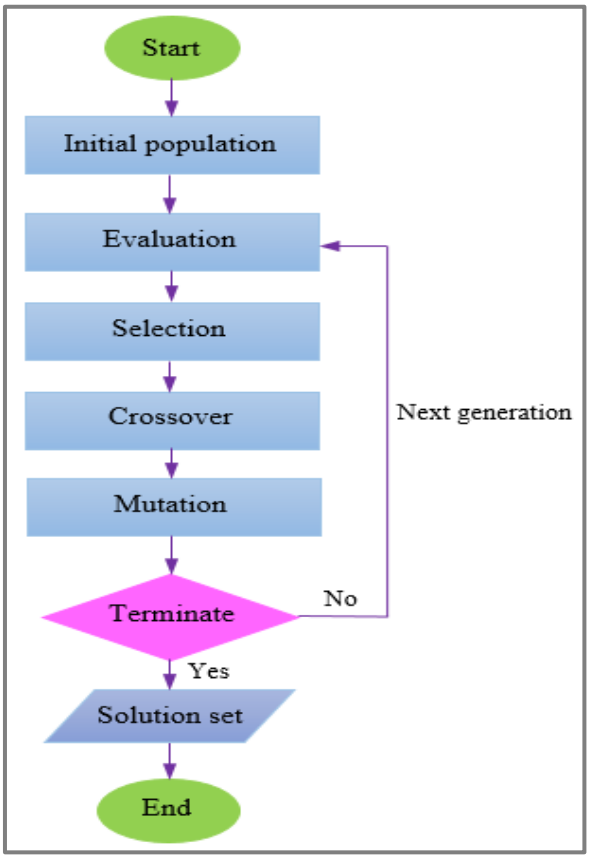

Fig.4: Flow chart of genetic algorithm for optimization

4. Proposed model

In order to correct Branson' s equation, one hundred twenty data have been used. These data, are the number of points on the load-deflection curve of hybrid FRP/steel RC beams with four-point loading. Using the genetic algorithm and available experimental data, Branson's equation has been modified so as to incorporate the slightest error than experimental values. The details of the experimental specimens used in table 1 are presented.

Table 1: experimental studies of hybrid Steel/FRP RC beams

Reference	Number of beam specimens	Number of data point	Type of FRP bar*
Aiello and Ombres (2002) [2]	4	29	AFRP
Qu et al (2009) [11]	6	46	GFRP
Leung and Balendran (2003) [28]	4	4	GFRP
Almusallam et al (2013) [29]	2	2	GFRP
Safan (2013) [30]	4	4	GFRP
Yang et al (2011) [31]	2	2	GFRP, CFRP
Sun et al (2012) [32]	1	1	BFRP
Refai et al (2015) [12]	6	33	GFRP

***AFRP** (aramid fiber reinforced polymer), **GFRP** (glass fiber reinforced polymer), **CFRP** (carbon fiber reinforced polymer), **BFRP** (basalt fiber reinforced polymer)

In this data, a wide range of specimens are presented in terms of changes in the modulus of elasticity of concrete and FRP bar, the compressive strength of concrete, the ultimate tensile strength of FRP bar, the yield strength of steel, the ratio of the area of FRP to steel rebar and different loading levels. Changes of these parameters are presented in table 2.

Table 2: The range of parameters changes in experimental data

Parameters	Minimum value	Maximum value
Modulus of elasticity of concrete (GPa)	24.9	40.94
Modulus of elasticity of FRP bar (GPa)	37.7	146
Compressive strength of concrete (MPa)	28.1	75.9
Ultimate tensile strength FRP bar (MPa)	743	2130
Yield strength of steel (MPa)	360	530
A_f/A_s	0.25	2.88

Experimental values of effective moment of inertia, $(I_e)_{exp}$ can be obtained by means of Eq. (26), using the values of mid span vertical displacement of the beam and its corresponding force.

$$(I_e)_{exp} = \frac{P_{exp}L_a}{48E_c\Delta_{exp}}(3L^2 - 4L_a^2) \quad (26)$$

Where Δ_{exp} is experimental mid span vertical deflection and P_{exp} is the experimental applied total load corresponding to Δ_{exp}.

After analyzing the parameters affecting the effective moment of inertia in Hybrid FRP / steel RC beams and comparing them with the effective moment of inertia of experimental data, the proposed formula is presented in equations (27) and (28).

$$(I_e)_{theo} = o.136\left(\frac{M_{cr}}{M_a}\right)^m I_g + 1.117\left(1 - \left(\frac{M_{cr}}{M_a}\right)^m\right) I_{cr} \quad (27)$$

$$m = 0.836\frac{E_f}{E_s} + 0.208\rho_{fb}\frac{A_f}{A_s} + 3.709\frac{M_{cr}}{M_a} \quad (28)$$

The equation (29) is introduced as an objective function and these coefficients are calculated by minimizing the error between the effective moment of inertia obtained from experimental result and equation (27).

$$e = \left|\frac{(I_e)_{theo} - (I_e)_{exp}}{(I_e)_{exp}}\right| \times 100 \quad (29)$$

In this section, by examining the sensitivity of m values to the change in the various factors, the effective parameters are identified in m values. Changes m are shown in Fig 5 to Fig 7 relation to different factors.

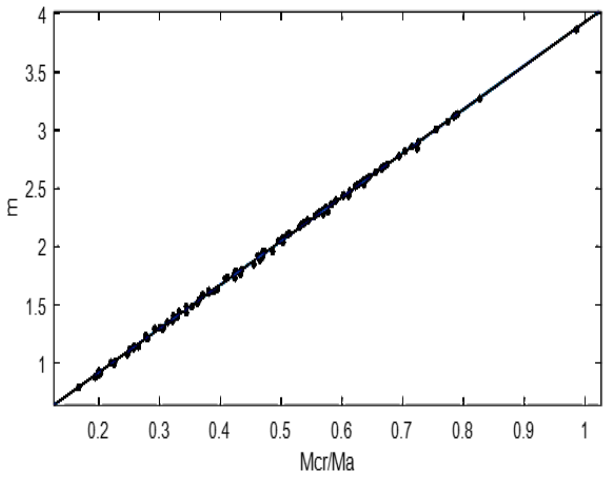

Fig.5: Relationship of m versus M_{cr} / M_a values

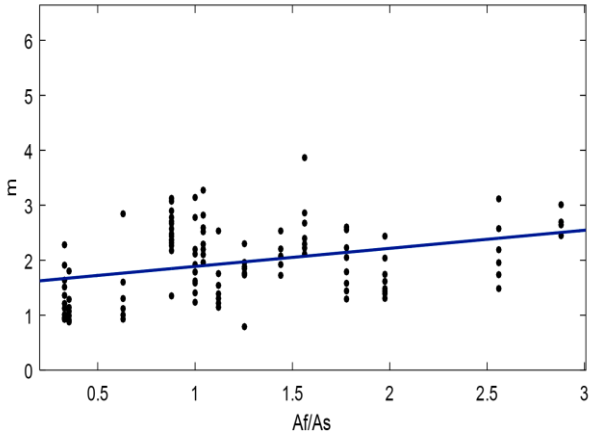

Fig.6: Relationship of m versus A_f / A_s values

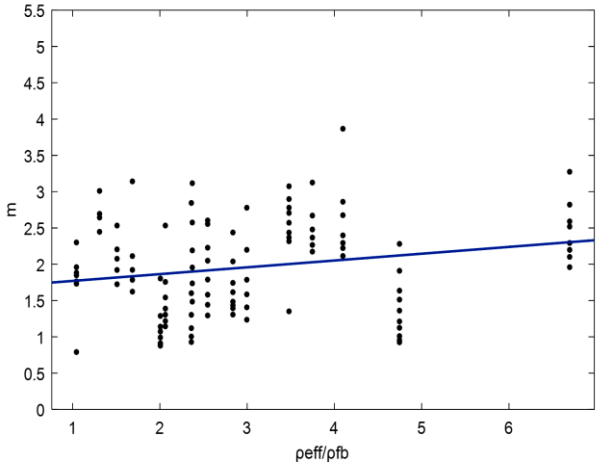

Fig.7: Relationship of m versus ρ_{eff} / ρ_{fb} values

Fig 8 and Fig 9 show that at high loading levels (low values of M_{cr} / M_a) and ratios with high reinforcement (large quantities ρ_{eff} / ρ_{fb}) due to the nonlinearity of concrete stresses, the value of the effective moment of inertia will be less than the cracked moment of inertia (I_{cr}). Therefore, parts of Branson' s equation must be multiplied by the coefficients of reduction in order to estimate the inertia value less than I_{cr}.

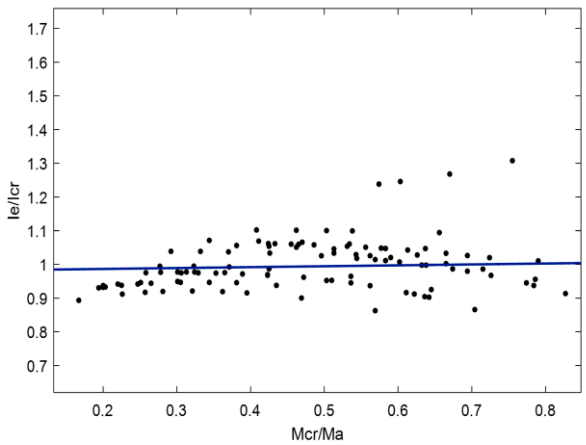

Fig.8: Relationship of I_e /I_{cr} versus M_{cr}/ M_a values

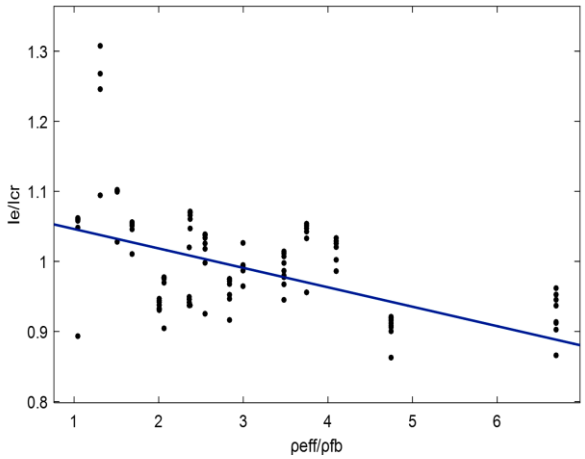

Fig.9: Relationship of I_e/I_{cr} versus ρ_{eff} / ρ_{fb} values

In order to verify the proposed equation, a statistical study was conducted on the deflection calculated from different models to experimental results. The mean values and standard deviation of data are shown in table (3).

Table 3: The range of parameters changes in experimental data

Model	mean	Standard deviation
Bischoff & Scanlon (2007) [33]	0.926	0.306
Benmokrane et al (1996) [23]	1.408	0.412
ACI 440.1R (2015) [22]	0.859	0.315
Branson(1965) [15]	0.8	0.376
Proposed model	1.189	0.377

According to this table, models with a mean of less than one are non-conservative with underestimated deflection. The results show that the proposed deflection model is conservative and accurately estimated. These values represent a good correlation between the proposed model and the experimental data compared to other methods.

The average error in 33 data with the random selection from the experimental database for the proposed model is equal to 5.7% while the average error for other models including Branson, ACI 440.1R-2015, Benmokrane et al and Bischoff & Scanlon is 32.65%, 24.81%, 20.38%, and 18.18 % respectively. In most specimens, the proposed equation shows a lower error percentage compared to other models. The prediction of the effective moment of inertia for the hybrid beams using an artificial neural network (Naderpour et al 2010[34]) has also been studying.

Conclusions

In this paper, at first, the experimental results of hybrid concrete beams reinforced with FRP and steel bars are compared to other equations of effective moment of inertia. On the basis of experimental response and Branson's equation, a new equation to calculate the effective moment of inertia in hybrid RC beams was proposed. By comparing the proposed model and other equations for the effective moment of inertia, the following results were obtained:

The proposed equation with consideration to the elasticity modulus ratio of FRP to steel bars and the ratio of the area of FRP to steel rebar has a higher accuracy compared to the previous equations.

Comparison between the results of the existing equation and the proposed equation with the experimental results showed that the proposed equation presents conservative values relative to the Branson, ACI 440 1R-2015, and Bischoff & Scanlon models.

The results of the study showed that the proposed equation using genetic algorithm had a lower percentage error in estimating the deflection of hybrid steel/FRP RC beams. The precision of the proposed equation was verified by available experimental data and showed good agreement.

References

[1] Dundar, C., Tanrikulu, A.K. and Frosch, R.J., 2015. Prediction of load–deflection behavior of multi-span FRP and steel reinforced concrete beams. Composite Structures, 132, pp.680-693.
[2] Aiello, M.A. and Ombres, L., 2002. Structural performances of concrete beams with hybrid (fiber-reinforced polymer-steel) reinforcements. Journal of Composites for Construction, 6(2), pp.133-140.
[3] Masmoudi, R., Theriault, M. and Benmokrane, B., 1998. Flexural behavior of concrete beams reinforced with deformed fiber reinforced plastic reinforcing rods. Structural Journal, 95(6), pp.665-676.
[4] Kocaoz, S., Samaranayake, V.A. and Nanni, A., 2005. Tensile characterization of glass FRP bars. Composites Part B: Engineering, 36(2), pp.127-134.
[5] Bakis, C.E., Nanni, A., Terosky, J.A. and Koehler, S.W., 2001. Self-monitoring, pseudo-ductile, hybrid FRP reinforcement rods for concrete applications. Composites science and technology, 61(6), pp.815-823.
[6] Jo, B.W., Tae, G.H. and Kwon, B.Y., 2004. Ductility evaluation of prestressed concrete beams with CFRP tendons. Journal of reinforced plastics and composites, 23(8), pp.843-859.
[7] Newhook, J.P., 2000. Design of under-reinforced concrete T-sections with GFRP reinforcement. In Proc., 3rd int. conf. on advanced composite materials in bridges and structures. Montreal: Canadian Society for Civil Engineering, pp. 153-60.
[8] Acciai, A., D'Ambrisi, A., De Stefano, M., Feo, L., Focacci, F. and Nudo, R., 2016. Experimental response of FRP reinforced members without transverse reinforcement: failure modes and design issues. Composites Part B: Engineering, 89, pp.397-407.
[9] Kara, I.F., Ashour, A.F. and Dundar, C., 2013. Deflection of concrete structures reinforced with FRP bars. Composites Part B: Engineering, 44(1), pp.375-384.
[10] Ge, W., Zhang, J., Cao, D. and Tu, Y., 2015. Flexural behaviors of hybrid concrete beams reinforced with BFRP bars and steel bars. Construction and Building Materials, 87, pp.28-37.

[11] Qu, W., Zhang, X. and Huang, H., 2009. Flexural behavior of concrete beams reinforced with hybrid (GFRP and steel) bars. Journal of Composites for construction, 13(5), pp.350-359.
[12] El Refai, A., Abed, F. and Al-Rahmani, A., 2015. Structural performance and serviceability of concrete beams reinforced with hybrid (GFRP and steel) bars. Construction and Building Materials, 96, pp.518-529.
[13] Pang, L., Qu, W., Zhu, P. and Xu, J., 2015. Design propositions for hybrid FRP-steel reinforced concrete beams. Journal of Composites for Construction, 20(4), p.04015086.
[14] Qin, R., Zhou, A. and Lau, D., 2017. Effect of reinforcement ratio on the flexural performance of hybrid FRP reinforced concrete beams. Composites Part B: Engineering, 108, pp.200-209.
[15] Branson, D.E., 1968, September. Design procedures for computing deflections. In Journal Proceedings, Vol. 65, No. 9, pp. 730-742.
[16] Yost, J.R., Gross, S.P. and Dinehart, D.W., 2003. Effective moment of inertia for glass fiber-reinforced polymer-reinforced concrete beams. Structural Journal, 100(6), pp.732-739.
[17] Bischoff, P.H., 2005. Reevaluation of deflection prediction for concrete beams reinforced with steel and fiber reinforced polymer bars. Journal of Structural Engineering, 131(5), pp.752-767.
[18] Kheyroddin, A. and Mirza, M.S., 1995. Flexural rigidity of reinforced concrete beams. In Canadian Society for Civil Engineering Annual Conference Proceedings, June (pp. 1-3).
[19] Kheyroddin, A., 1996. Nonlinear Finite Element Analysis of Flexure- Dominant Reinforced Concrete Structures, Ph.D. Thesis, Department of Civil Engineering and Applied Mechanics, McGill University, Montreal, Canada, 290p.
[20] Shayanfar, M.A., Kheyroddin, A., and Mirza, M.S. 1997. Element Size Effects in Nonlinear Analysis of Reinforced Concrete Members, Computers & Structures, 62(2), pp.339-352.
[21] Bischoff, P.H., 2007. Deflection calculation of FRP reinforced concrete beams based on modifications to the existing Branson equation. Journal of Composites for Construction, 11(1), pp.4-14.
[22] ACI 440.1R. 2015. Guide for the design and construction of structural concrete reinforced with FRP bars. American Concrete Institute, Farmington Hills.
[23] Benmokrane, B., Chaallal, O. and Masmoudi, R., 1996. Flexural response of concrete beams reinforced with FRP reinforcing bars. ACI Structural Journal, 93(1), pp.46-55.
[24] Mousavi, S.R. and Esfahani, M.R., 2012. Effective moment of inertia prediction of FRP-reinforced concrete beams based on experimental results. Journal of Composites for Construction, 16(5), pp.490-498.
[25] CAN, C.S., 2012. CSA-S806-12. Design and construction of building components with fiber-reinforced polymers. Mississauga, Ontario, Canada: Canadian Standards Association.
[26] Goldberg, D.E., 1989. Genetic algorithms in search, optimization, and machine learning, 1989. Reading: Addison-Wesley.
[27] Bodenhofer, U., 2003. Genetic algorithms: theory and applications.
[28] Leung, H.Y. and Balendran, R.V., 2003. Flexural behaviour of concrete beams internally reinforced with GFRP rods and steel rebars. Structural Survey, 21(4), pp.146-157.
[29] Almusallam, T.H., Elsanadedy, H.M., Al-Salloum, Y.A. and Alsayed, S.H., 2013. Experimental and numerical investigation for the flexural strengthening of RC beams using near-surface mounted steel or GFRP bars. Construction and Building Materials, 40, pp.145-161.
[30] Safan, M.A., 2013. Flexural Behavior and Design of Steel-GFRP Reinforced Concrete Beams. ACI Materials Journal, 110(6).
[31] Yang, J.M., Min, K.H., Shin, H.O. and Yoon, Y.S., 2011. Behavior of high-strength concrete beams reinforced with different types of flexural reinforcement and fiber. In Advances in FRP Composites in Civil Engineering ,pp. 275-278.
[32] Sun, Z.Y., Yang, Y., Qin, W.H., Ren, S.T. and Wu, G., 2012. Experimental study on flexural behavior of concrete beams reinforced by steel-fiber reinforced polymer composite bars. Journal of Reinforced Plastics and Composites, 31(24), pp.1737-1745.
[33] Bischoff, P.H. and Scanlon, A., 2007. Effective moment of inertia for calculating deflections of concrete members containing steel reinforcement and fiber-reinforced polymer reinforcement. ACI Structural Journal, 104(1), p.68.
[34] Naderpour, H., Kheyroddin, A. and Amiri, G.G., 2010. Prediction of FRP-confined compressive strength of concrete using artificial neural networks. Composite Structures, 92(12), pp.2817-2829.